Metal Recovery from Hydroprocessing Spent Catalyst: A Green Chemical Engineering Approach

ARTICLE *in* INDUSTRIAL & ENGINEERING CHEMISTRY RESEARCH · NOVEMBER 2013

Impact Factor: 2.59 · DOI: 10.1021/ie4024484

3 AUTHORS, INCLUDING:

Garima Chauhan
Guru Gobind Singh Indraprastha University
11 PUBLICATIONS **55** CITATIONS

SEE PROFILE

K.K. Pant
Indian Institute of Technology Delhi
37 PUBLICATIONS **803** CITATIONS

SEE PROFILE

I&EC research
Industrial & Engineering Chemistry Research

Article

pubs.acs.org/IECR

Metal Recovery from Hydroprocessing Spent Catalyst: A Green Chemical Engineering Approach

Garima Chauhan, Kamal K. Pant, and Krishna D. P. Nigam*

Department of Chemical Engineering, Indian Institute of Technology, IIT Delhi, Hauz Khas, New Delhi, Delhi -110016, India

Supporting Information

ABSTRACT: The present study aims to develop an ecofriendly, chelant-assisted extraction methodology for significant recovery of heavy metals (cobalt (Co), molybdenum (Mo)) from hydroprocessing spent catalyst. Ethylene diamine tetraacetic acid (EDTA) was employed for metal mobilization in the extraction process. The possibility of internal and external mass transfer resistance was investigated to improve the diffusion rate of reactants, while kinetic aspects were studied to achieve thermodynamic equilibrium for the process. Percentage distribution of various protonation stages of EDTA was explored to understand the conjugate base and ligand precursor and to improve the effect of reaction pH on extraction efficiency. Extraction of 80.4% Co and 84.9% Mo was achieved at optimum reaction conditions. Selective precipitation of metals was attained according to maximum solubility of metal oxides at different pH regions. Efforts were also made to recycle the recovered EDTA, recovered support material, and extracted metals. Significant metal extraction efficiency (72.7% Co and 76.5% Mo) was observed with recovered EDTA even after the fourth cycle of operation which may provide economic consistency to the extraction process. The extracted metals were impregnated on recovered alumina to synthesize fresh catalyst. Structural analysis of spent catalyst, recovered support material, and synthesized catalyst from extracted metals suggested successful recovery and recycling of metals. This work offers an incentive to the industrial practice for waste minimization, recycling of the extracted metals, and the noncorrosive, ecofriendly approach for metal extraction from spent catalyst.

1. INTRODUCTION

Fast-paced demographic and economic developments throughout the world significantly contribute to the rising levels of resource consumption. Many of these resources are at the risk of critical scarcity in the coming years, while others have already become less abundant relative to necessity. Since it is pragmatically impossible to increase resource consumption efficiencies indefinitely, it is equally inconceivable to have an infinite economic and industrial growth without a concomitant increase in resource depletion and environmental pollution. Therefore, there is an urgent need to achieve resource sustainability by improving the resource intensity with amelioration in existing technology as well as minimizing the negative impact of the industrial development on the environment.

Economic development is closely linked to the use of metals for industrial activities such as petrochemicals, fertilizer, construction, transport, and communication sectors. A report by the International Resource Panel, United Nations Environment Programme (UNEP) suggests that the global in-use stocks of metals are expected to grow 3−9-fold in the coming years.[1] This incessant increasing need of metals may create a gap between demand and supply of metals. Concurrently, large amounts of industrial wastes such as spent catalyst are generated from hydroprocessing industries which contain a substantial quantity of heavy metals and may affect the ecosystem and living organisms if not disposed of in a proper manner. Recovery and recycling of heavy metals may become a considerable solution to minimize the industrial waste as well as to overcome the scarcity of the metals. The literature suggests that metal extraction from spent catalysts can be performed using either hydrometallurgical or pyrometallurgical methods. Pyrometallurgical processes such as calcination to remove the coke, sulfur, and other foulants, followed by leaching with alkali reagent[2,3] or roasting of spent catalyst with suitable reagents at high temperatures[4,5] have been studied extensively for the recovery of molybdenum (Mo) from spent catalyst. Several hydrometallurgical approaches have also been reported[6−9] to recover metals from spent catalyst, soil, and other industrial waste. Mishra and co-workers[7] used leaching solvent extraction techniques to recover nickel (Ni), vanadium(V), and Mo from spent petroleum catalyst. Park and co-workers[10] investigated the selective extraction of high-purity MoO_3 from spent hydrodesulfurization catalyst using a mixture of Na_2CO_3 and H_2O_2. Santhiya and Ting[11] performed one-step and two-step bioleaching processes for treating spent hydroprocessing catalyst containing Ni and Mo as major components. All these physicochemical processes have shown potential in removing metals from spent catalyst; however, process cost, large amounts of chemicals needed, disposal of the chemicals, secondary pollution possibility by these chemicals, and less acceptance of biological process in the environment restrict their use on large scale. Chelation technology can be employed for metal extraction from spent catalyst at relatively lower temperatures, and the chelating agents can be reused in the extraction process itself.[12−14] Performance of the biodegradable chelating agent [*S*,*S*]-ethylenediamine disuccinic acid ([*S*,*S*]-

Received: July 29, 2013
Revised: October 3, 2013
Accepted: November 4, 2013

   dx.doi.org/10.1021/ie4024484 | *Ind. Eng. Chem. Res.* XXXX, XXX, XXX−XXX

EDDS) was investigated for nickel extraction from spent catalyst, and comparable efficiency was observed for [*S*,*S*]-EDDS and conventional chelating agent ethylene diamine tetraacetic acid (EDTA).[12] Goel and co-workers[13] employed EDTA for recovery of Ni metal from spent catalyst and 96% nickel was recovered in the form of nickel sulfate with fresh EDTA concentration 0.8 M, reaction time 10 h, temperature 100 °C, and pH 10. Vuyyuru and co-workers[14] achieved 95% Ni recovery using EDTA under hydrothermal reaction conditions in an autoclave, at temperatures of 150 °C, over a 4 h period. Easy recovery of chelating agent, noncorrosive environment, and absence of any hazardous byproducts during the process are the convincing factors which make this technology more favorable than other available technologies for metal recovery.

Chelant-assisted metal extraction is assumed to occur at the solid−liquid interface. When chelating agents (L^{-4}) are introduced to the solid−liquid interface, formation of metal−chelant complexes takes place on the catalyst surface by surface complexation. These metal complexes (M_i−L^{-2}) are dissociated from the solid surface into solution as shown in eq 1. Here M_i^{+2} refers to the metal of interest with which the ligand interact, {[HDS]-O} represents sorption sites on the catalyst surfaces, and M_{ii}^{+2} denotes other metals present in solution. Metal oxides and hydroxides, if present, are also partially dissolved by ligand-promoted dissolution (eqs 2 and 3).[15,16]

$$\{[HDS]-O\} - M_i^{+2} + L^{-4} + H_2O \leftrightarrow [HDS]-OH + M_i - L^{-2} + OH^- \quad (1)$$

$$M_i(OH)_2 + L^{-4} \leftrightarrow M_i - L^{-2} + 2OH^- \quad (2)$$

$$M_iO + L^{-4} + H_2O \leftrightarrow M_i - L^{-2} + 2OH^- \quad (3)$$

Some of the metal−chelant complexes still remain in contact with the catalyst surfaces. They may be readsorbed via surface complexation (eq 4) or exchanged with other sorbed metals (M_{ii}^{+2}) as shown in eqs 5 and 6, depending on the stability constants of metal−chelant complexes, binding strength of M_i^{+2} on the surface, and accessibility of M_{ii}^{+2}.[15,17,18]

$$[HDS]-OH + M_i - L^{-2} \leftrightarrow [HDS]-L-M_i + OH^- \quad (4)$$

$$[HDS]-L-M_i + [HDS]-O-M_{ii}^{+} \leftrightarrow [HDS]-L-M_{ii} + [HDS]-OH + M_i^{+} \quad (5)$$

$$[HDS]-L-M_{ii} + OH^- \leftrightarrow [HDS]-OH + M_{ii} - L^{-2} \quad (6)$$

The present study explores an innovative combination of chelation and dechelation processes for the extraction of cobalt (Co) and molybdenum (Mo) metals from hydroprocessing spent catalyst. The focus has been to obtain the individual metals in solution on the basis of maximum solubility of metal oxides at different pH range. Efforts were also made to recycle the extracted metals and alumina support material for synthesis of new catalysts. Reaction parameters were optimized under autogenous reaction conditions to achieve higher conversion, and results were compared with the atmospheric reflux conditions. Waste minimization, reutilization of the extracted metals, and the noncorrosive nature of the extraction process offer a great incentive to the industrial practice.

2. MATERIALS AND METHODS

2.1. Spent Catalyst. The secondary reforming hydrodesulfurization spent catalyst used in the present study was provided by a fertilizer industry (Indian Farmers Fertiliser Cooperative Limited (IFFCO)) India. Elemental composition of the catalyst was determined using inductively coupled plasma optical emission spectrometry (ICP-OES) analysis. ICP-OES analysis illustrated 8.7% Mo, 2.6% Co with the balance being the support material γ-Al_2O_3 and other minor impurities such as coke and sulfur. Characterization techniques were adopted for the evaluation of physicochemical properties of spent catalyst. Thermogravimetric analysis (TGA) of spent catalyst was carried out using a TGA/DTA simultaneous thermal analyzer apparatus STT-Q-600 from TA Instruments under flow of oxygen gas. Specific surface area and pore volume were determined using Micrometrics adsorption equipment (ASAP 2010), whereas a tapping method (Tap Density Tester, Lab India, TD 1025) was used for the density measurement. The morphology of the catalyst sample was investigated using a scanning electron microscope (SEM) EVO50 and energy dispersive X-ray (EDX) analysis was performed to confirm the elemental composition. X-ray diffraction (XRD) patterns were collected with a step size of 0.05° over the range $10° < 2\theta < 90°$ using Philips X'pert-1 X-ray diffractometer to investigate the crystalline phases of the samples.

2.2. UV Spectrophotometric Analysis. The metal concentration in solution was analyzed using a Cary 5000 Varian UV spectrophotometer fitted with quartz cells. Absorbance for Co metal was recorded at a wavelength of 513 nm, and the unknown concentration of Co in the solution was calculated. However, Mo cannot be analyzed in UV spectrophotometer without employing any chromogenic reagent; therefore, spectrophotometric determination of Mo was performed using synthesized reagent cinnamaldehyde-4-hydroxybenzoylhydrazone (CHBH) crystals as mentioned in the literature.[19] CHBH crystals were prepared by mixing a suitable quantity of cinnamaldehyde and 4-hydroxybenzahydrazide into a sufficient amount of methanol. The mixture was refluxed for 4 h and recrystallized twice using hot methanol to obtain pure, light-yellow crystals of CHBH. Fourier transform infrared (FT-IR) (Thermoscientific, Nicolet 6700) and nuclear magnetic resonance (NMR) (Bruker AC 300 nuclear magnetic resonance spectrometer (300 MHz FT-NMR)) spectral studies were performed to characterize the compound. Spectrophotometric analysis of Mo was performed using 0.01 M of CHBH reagent solution as explained in the literature[19] with minor modifications. Reagent solution (0.01 M) was prepared by dissolving CHBH crystals into 100.0 mL of dimethylformamide (DMF). Standard solutions of different concentrations of Mo were prepared by dissolving sufficient amounts of $Na_2MoO_4 \cdot 2H_2O$ in 3.0 mL of buffer solution (0.1 M potassium dihydrogen phosphate + 0.1 M sodium hydroxide, pH 5.0) with the addition of 0.5 mL of CHBH solution, and the volume was made up to 20.0 mL by adding the requisite amount of distilled water. The unknown concentration of Mo in the solution was calculated based on the absorbance of each solution for Mo metal.

2.3. Chelation Studies under Autogenous Reaction Conditions. The experimental procedure includes the pretreatment (comminution and calcination) of spent catalyst as the first step of chelant-assisted metal extraction process. The calcination temperature was determined by thermogravimetric

dx.doi.org/10.1021/ie4024484 | Ind. Eng. Chem. Res. XXXX, XXX, XXX−XXX

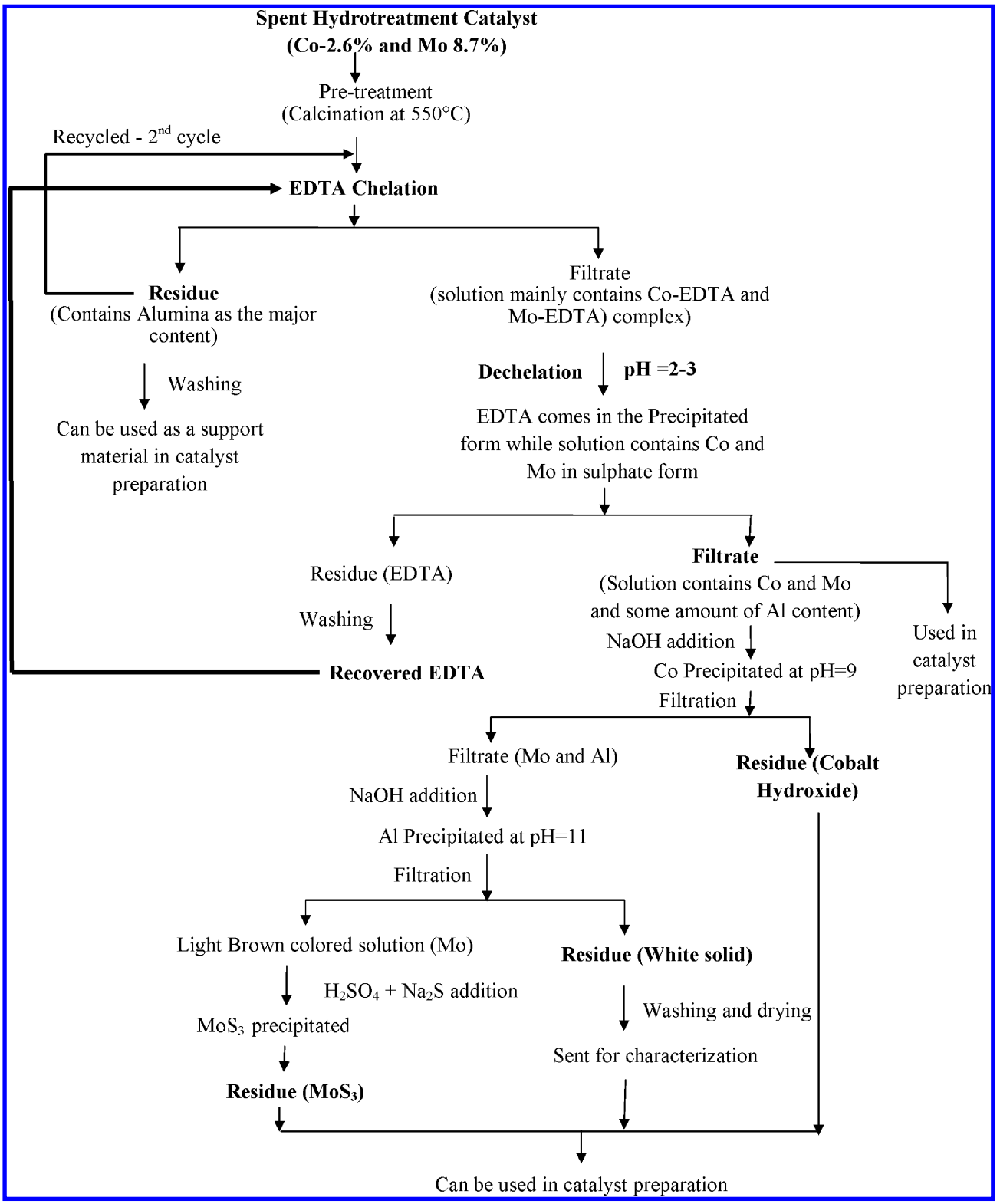

Figure 1. Proposed methodology of chelant-assisted metal extraction from spent catalyst and possibility of their reutilization in catalyst preparation.

analysis of spent catalyst for which the sample (10 mg) was heated from 50 to 800 °C at the heating rate of 10 °C/min under flow of oxygen gas. TGA-DTA analysis demonstrated a gradual weight change upon heating from 50 to 500 °C; however, after attaining 500 °C temperature, the catalyst was observed to be thermally stable up to 800 °C without significant weight reduction. Therefore, the catalyst was calcined in the presence of atmospheric oxygen flow in a temperature-controlled muffle furnace for 5 h at 500 °C to remove coke and other impurities. The mass loss was about 7–9 wt % for the catalyst after the pretreatment of spent catalyst which confirms the removal of coke and other impurities from the catalyst surface. The proposed process flowchart for

dx.doi.org/10.1021/ie4024484 | Ind. Eng. Chem. Res. XXXX, XXX, XXX–XXX

Table 1. Functional Groups for CHBH Crystals Corresponding to the Transmission Peaks

functional groups	transmission peak (cm^{-1}) - present study	transmission peak (cm^{-1})[19]
amine salts (−NH Stretching)	3448	3452
−OH groups	3264, 3031	3218−3092
symmetric stretching of carboxylate groups	2358, 2021	–
asymmetric stretching of the carboxylate group (−C═O)	1622	1620
CH bending and C−N stretching (C═N)	1576, 1500−1300	1577
═C−H bend alkenes/aromatics	1211	–
C−O stretch alcohols, carboxylic acids	974	–
−C−H rock alkanes	899	–
hydroxyl complexes	750	–

recovery and reutilization of extracted metals is presented in Figure 1.

Chelation experiments were conducted with 10 g of spent catalyst in a closed batch reactor under autogenous reaction conditions. Ethylene diamine tetraacetic acid (EDTA) with a wide range of molar concentration (0.1−0.6 M) and solid to liquid ratio (S/L) (1/5 to 1/25) was employed as a chelating agent due to its better extraction efficiency and reusability over other aminopolycarboxylates[12−14,20] and its commercial availability. NaOH solution (0.1 M) was added dropwise to maintain a basic pH of the solution so that EDTA would dissolve completely in distilled water. After a certain reaction time, the slurry was collected and filtered through Whatmann filter paper of 150 mm diameter in a funnel with porous disc (pore size 40−90 μ, porosity grade 2) using a vacuum pump. The residue material (alumina) was separated from the complex solution, and the filtrate (dark-pink color) was sent for the dechelation process where the metal−chelate complex was hydrolyzed by lowering the pH of solution to induce the precipitation of the chelating agent.[14] Precipitated EDTA was filtered from the solution which can be reused for extraction process after washing with distilled water (4 mL/g precipitated solid) at 60 °C temperature and then drying at 100 °C for 2 h. Solution was then treated for the selective precipitation of Co and Mo on the basis of maximum solubility of metal oxides at different pH ranges. Mo present in a low Co concentration solution could be precipitated in an efficient way compared with a high cobalt concentration solution. When Co is present in higher concentration in the solution, then coprecipitation of Co and Mo takes place at acidic pH, while as the solution pH moves toward alkaline conditions, Mo redissolves in the solution and only Co can be precipitated.[21] Therefore, Co was precipitated first to avoid any coprecipiation of Co with Mo. Cobalt was recovered at pH = 9 by the slow addition of NaOH (2 N) at room temperature. After filtration, the solution pH was increased further up to pH = 11 to precipitate the aluminum present in solution. The precipitate was separated from the solution and washed with water (4 mL/g solid) to remove any impurities. The solid material of pure white color was then dried at 150 °C and sent for characterization (XRD, EDX, ICP-OES analysis). The light-brown colored solution, left after the filtration, was reduced to near 40% of the initial volume by evaporative heating as mentioned in the literature[22] which helps to precipitate Na_2MoO_4 partially. The precipitate was filtered and resolubilized with water at room temperature (6 mL/g solid). Then Na_2S (2 mol/L) was added to the solution, and the pH was maintained at a pH = 6.5−7 for a period of one hour to convert molybdenum in the form of tetrathiomolybdate. The thiomolybdate ion is soluble in basic solution, and molybdenum trisulfide does not precipitate until the solution is made acidic;[23] therefore, sulfuric acid was added to the solution at 80−90 °C to maintain solution pH = 3. The chemistry associated with the precipitation of molybdenum sulfide is given as follows in eqs 7 and 8:[23]

$$MoO_4^- + 4S^- + 4H_2O \rightarrow MoS_4^- + 8OH^- \quad (7)$$

$$MoS_4^- + 8OH^- + 5H_2SO_4 \rightarrow MoS_3 + H_2S + 8H_2O + 5SO_4 \quad (8)$$

The precipitate (dark-brown color) was filtered and washed with H_2SO_4 (0.2 N), followed by washing with water at 60 °C (4 mL/g) solid) to remove any impurities. Precipitate (molybdenum trisulfide) was roasted in atmospheric oxygen flow at 500 °C for oxidizing MoS_3 to molybdate. Characterization (XRD, EDX, and ICP-OES) confirmed the recovery of Mo metal with 91% purity in the form of molybdate. The extracted metals were investigated for the possibility of metal recycling in preparation of new fresh catalyst.

The amount of metal (Co/Mo) extracted is given as the ratio of metal present in solution to metal initially present in the spent catalyst. Percentage (%) extraction of Co or Mo is defined explicitly as follows:

$$(\%)\ \text{extraction of metals Co/Mo} = \frac{(\text{metals present in solution})}{(\text{metals initially present in spent catalyst})} * 100$$

Effect of various process parameters (stirring speed, particle size, reaction temperature, reaction time, solid to liquid ratio, molar concentration of EDTA, pH) on metal extraction were investigated to attain the optimized reaction conditions.

2.4. Structural Analysis of Recovered Material. Recovered support material alumina obtained in the form of residue after the chelation−dechelation process and the extracted metals present in the solution were again used for preparation of new fresh catalyst. Various characterization procedures (BET, XRD, SEM and EDX as mentioned in the Spent Catalyst section) were adopted to investigate the recycling of recovered metals. EDTA, the chelating agent used in the present study, was also recovered by means of the dechelation process. Fresh EDTA and recovered EDTA(s) were characterized using FT-IR and NMR spectral studies, and results were compared to investigate any structural changes or presence of impurities in recovered EDTA.

3. RESULTS AND DISCUSSIONS

3.1. Characterization of CHBH Crystals. Fourier transform infrared (FT-IR) spectrum analysis was performed for the characterization of cinnamaldehyde-4-hydroxybenzoylhydra-

dx.doi.org/10.1021/ie4024484 | Ind. Eng. Chem. Res. XXXX, XXX, XXX−XXX

zone (CHBH) crystals. Pellets were prepared by mixing 0.5 g of CHBH crystals in sufficient amount of potassium bromide (KBr). Various functional groups determined from the infrared spectrum of the CHBH crystals are listed in Table 1. The data was compared with the available literature on corresponding transmission peaks. It can be depicted from Table 1 that CHBH crystals have bands at different wave numbers for functional groups such as −OH, -C═O, -NH, phenolic etc. The transmission peaks obtained for the prepared crystal at different wave numbers were found to be in good agreement with the available literature.[19]

Nuclear magnetic resonance (NMR) spectroscopy was carried out to confirm the structure of CHBH crystals. The sample was prepared in dimethyl sulfoxide (DMSO) solvent for the ^{1}H NMR (300 MHz) spectrum of the reagent. The ^{1}H NMR spectrum and molecular formula of CHBH crystals are shown in Figure 2. The NMR spectrum demonstrated the

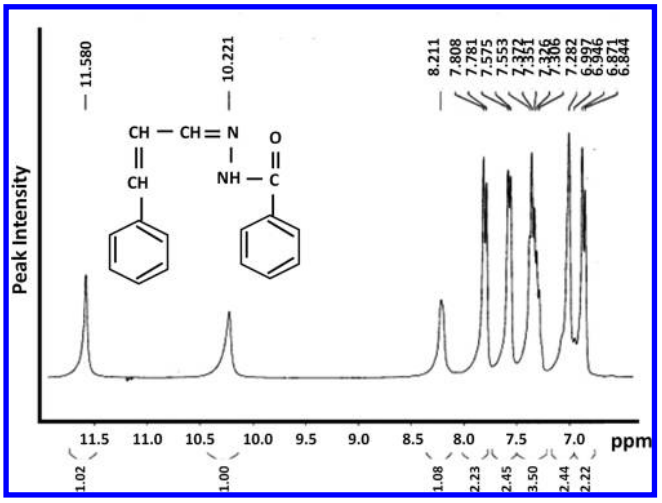

Figure 2. Nuclear magnetic spectrum (^{1}H) of prepared CHBH crystal.

signals corresponding to δ 11.58 (s, 1H, −NH), 10.22 (s, 1H, −OH phenolic), 8.21 (s, 1H, N−CH), 7.78−7.80 (d, 2H, ArH), 7.55−7.57(d, 2H, ArH), 7.30−7.35 (m, 3H, ArH), 6.95−6.99 (d, 2H, ArH). All the peaks were observed in concordance with the peak signal reported in the literature;[19] thus, formation of CHBH crystals was confirmed.

3.2. Possible Mass Transfer Limitation in Chelant-Assisted Extraction Process. Stirring speed of an agitator and particle size distribution are important factors for the consideration of mass transfer from solid phase to liquid phase in the metal extraction process. Verification of external mass transfer as the rate-limiting step was accomplished by varying the stirring speed of an agitator for a wide range of 100−600 rpm at molar concentration of EDTA = 0.4 M, solid to liquid (S/L) ratio = 1/15 (w/v), reaction temperature = 120 °C, reaction time = 4 h, particle size = 300 μm, and pH = 9. Co and Mo extraction increase with an increase in stirring speed; however, beyond a stirring speed of 400 rpm, external mass transfer resistance does not affect the process rate significantly (Figure 1 in Supporting Information [SI]). Only 3−5% improvement in extraction efficiency was observed with the increase in stirring speed beyond 400 rpm; therefore, 400 rpm was considered as the optimum stirring speed for further metal extraction experiments.

Particle size distribution, which is indicative of the power consumed during the comminution process, was also investigated to study the effect the internal mass transfer resistance. The particle size distribution was measured using sieve analysis with a set of standard sieves and different particle sizes ranging <100 μm, 100−300 μm, 300−500 μm, 500−800 μm, and >800 μm were employed for the extraction process. Nearly 30−35% increase in extraction efficiency was observed for both the metals with reduction in particle size from 800 to 100 μm (Figure 2 in SI). A significant effect of particle size on % metal extraction efficiency substantiated the dominance of internal diffusion on extraction process.[12] However, there was not a significant increase in extraction efficiency below particle size range of 100−300 μm; therefore, internal mass-transport resistance (diffusion in the pores of the particles) can be disregarded below the specified particle size range of 100−300 μm. Particle size range of 100−300 μm was taken as the optimum particle size of spent catalyst for further experiments on the basis of the experimental data obtained for the reduction of particle size.

3.3. Kinetic Aspects of the Chelant-Assisted Metal Extraction Process. It was necessary to achieve the thermodynamic equilibrium for the optimization of metal extraction process. Therefore, experiments were performed in a batch autoclave at different reaction temperatures (100−140 °C) for different reaction times (1−6 h) to study the effect of reaction temperature and reaction time on extraction efficiency where other reaction parameters were kept constant: molar concentration of EDTA = 0.4 M, S/L ratio of 1/15, and a particle size range of 100−300 μm, pH = 9, and stirring speed of 400 rpm. Initial reaction rates were calculated for different process parameters to substantiate the claim of operating conditions.[12] A and B of Figure 3 demonstrate the effect of reaction temperature on the Co/Mo extraction at different reaction times. It can be seen from Figure 3A that extraction efficiency increases with increase in reaction temperature and attains an asymptotic value (Co 80.4% and Mo 84.9%) at a reaction temperature of 120 °C within 4 h of reaction time. The increase in (%) metal extraction with increase in temperature may be explained on the basis of the possibility of enhanced reaction kinetics due to Arrhenius behavior of the surface reaction that dissolves the metal. Another observation related to autogenous reaction conditions suggests that, with the increase in temperature under batch autoclave, pressure also increased and reached up to 2.7 atm at temperature 140 °C which favors the rate of the forward reaction; hence, metal extraction efficiency improves. A similar extraction process was also operated under atmospheric reflux conditions at a reaction temperature 100 °C, and about 58% Mo was extracted which was nearly 12% less than the extraction efficiency obtained under autogenous conditions. Moreover, the chelation step would take place in stirred autoclaves in a practical industrial plant. Thus, it can be concluded that the chelant-assisted extraction process under atmospheric reflux conditions is neither optimal nor practically feasible on an industrial platform.[14] Therefore, autogenous reaction conditions were considered more favorably to optimize extraction efficiency. A plot of initial reaction rates vs reaction temperature is shown in Figure 3B. It can be seen from Figure 3B that, at a given reaction time, an increase in the initial reaction rate was observed with the increase in reaction temperature; however, the initial reaction rate becomes nearly constant at the temperature 120 °C; therefore, the reaction temperature of 120 °C was considered optimum for the metal extraction process. The amount of metal extracted attains an asymptotic

dx.doi.org/10.1021/ie4024484 | Ind. Eng. Chem. Res. XXXX, XXX, XXX−XXX

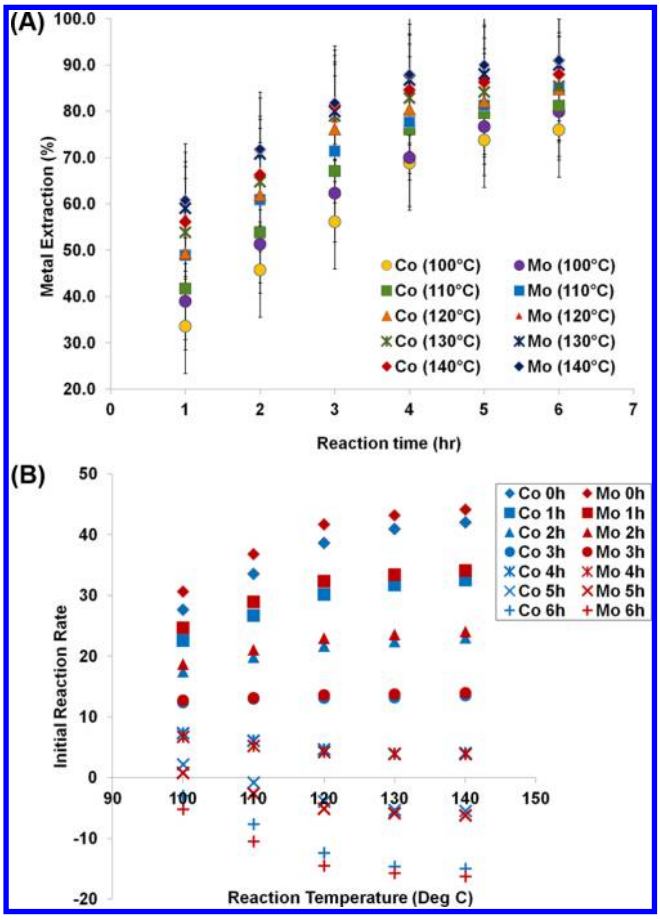

Figure 3. (A) Effect of reaction temperature and reaction time on (%) metal extraction (reaction conditions: molar concentration of EDTA = 0.4 M, S/L = 1/15, particle size = 100−300 μm, stirring speed = 400 rpm, pH = 9). (B) Plot of initial reaction rate vs reaction temperature.

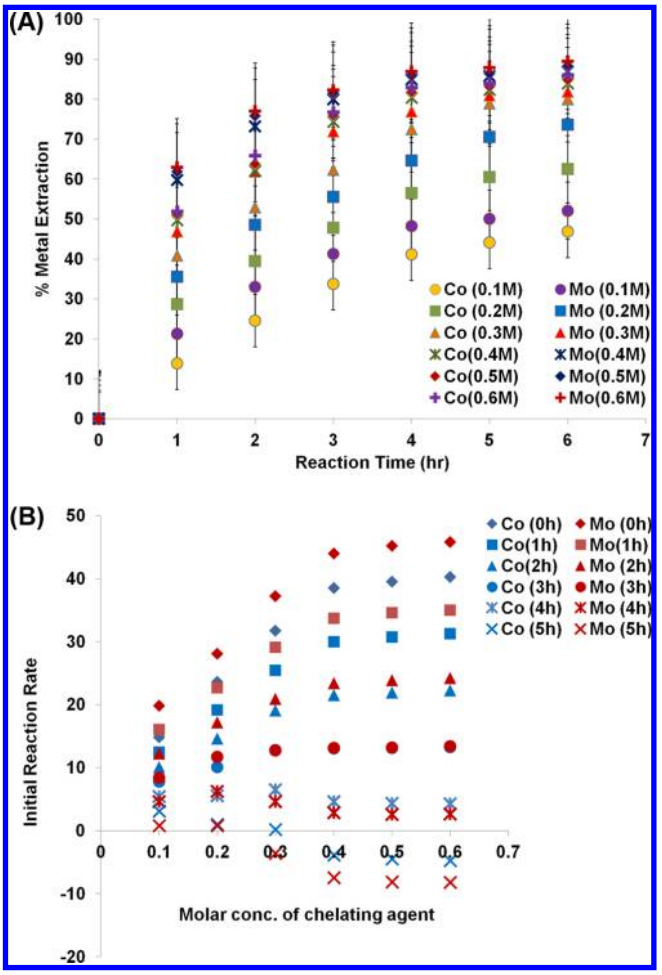

Figure 4. (A) Effect of molar concentration of EDTA on metal extraction efficiency (reaction conditions: S/L = 1/15, temperature = 120 °C, time = 4 h, particle size = 100−300 μM, stirring speed = 400 rpm, pH = 9). (B) Plot of initial reaction rate vs molar concentration of chelating agent.

value at 4 h of reaction time, and thus 4 h was considered as the optimum reaction time for metal extraction.

Kinetic aspects were studied in further experiments on the prescribed operating conditions by varying the molar concentration of EDTA and S/L ratio. The kinetic extraction experiments were carried out at different molar concentrations of EDTA varying from 0.1 M to 0.6 M. A and B of Figure 4 depict the kinetic extraction of Co and Mo metals using chelating agent EDTA. It may be observed from Figure 4A that extraction efficiency increases with the increase in molar concentration of EDTA from 0.1 M to 0.6 M. At molar concentration of 0.4 M, the amount of extracted Co/Mo reaches a plateau which corresponds to the maximum extractable quantity. An excess of molar concentration of chelating agent (0.6 M) did not show any significant increase in extraction efficiency beyond molar concentration of 0.4 M. Similar observations can also be seen from Figure 4B which shows a plot of molar concentration of chelating agent vs initial reaction rate. It can be concluded from Figure 4B that the initial reaction rate becomes nearly constant at molar concentration of 0.4 M and therefore, 0.4 M was considered as the optimum molar concentration of EDTA to maximize the extraction efficiency of chelating agent.

Molar ratio of EDTA to metal (MR) was also calculated for different molar concentrations of EDTA at S/L=1/15, and one set of experiments was conducted at MR = 1:1 (molar concentration of EDTA = 0.03 M for Co, 0.06 M for Mo). At molar concentration of EDTA = 0.06 M, extraction efficiency of EDTA was not significant (below 20% for both the metals) after 4 h of reaction time at temperature 120 °C under autogenous conditions. It may be concluded from the above observations that the chelant concentration should be above the stoichiometric amount to attain higher percentage of extractable metals. Similar observations were also reported in the literature[20] where extraction of Ni from spent catalyst was not found to be appreciable at low concentration (MR = 1.2) of the chelating agents EDTA, DTPA, and [*S*,*S*]-EDDS.

Similar kinetics were observed when keeping the molar concentration of EDTA constant at 0.4 M and S/L was varied from S/L = 1/5 to S/L = 1/25 as shown in A and B of Figure 5. Using the S/L = 1/5, very small amounts of metals (28.7% Co and 34.7% Mo) were extracted from the spent catalyst due to a low reaction rate. It was observed that extraction efficiency improves with an increase in the amount of extractant solution and reached up to 84.9% Mo and 80.4% Co at S/L = 1/15 g/mL and pH = 9. Further increase in extractant solution could not make a significant change in the Co/Mo recovery; additionally, a large amount of reactant (chelating agent) has to be used for higher S/L which is not economically feasible. Therefore, S/L = 1/15 is regarded as the optimum ratio with

dx.doi.org/10.1021/ie4024484 | *Ind. Eng. Chem. Res.* XXXX, XXX, XXX−XXX

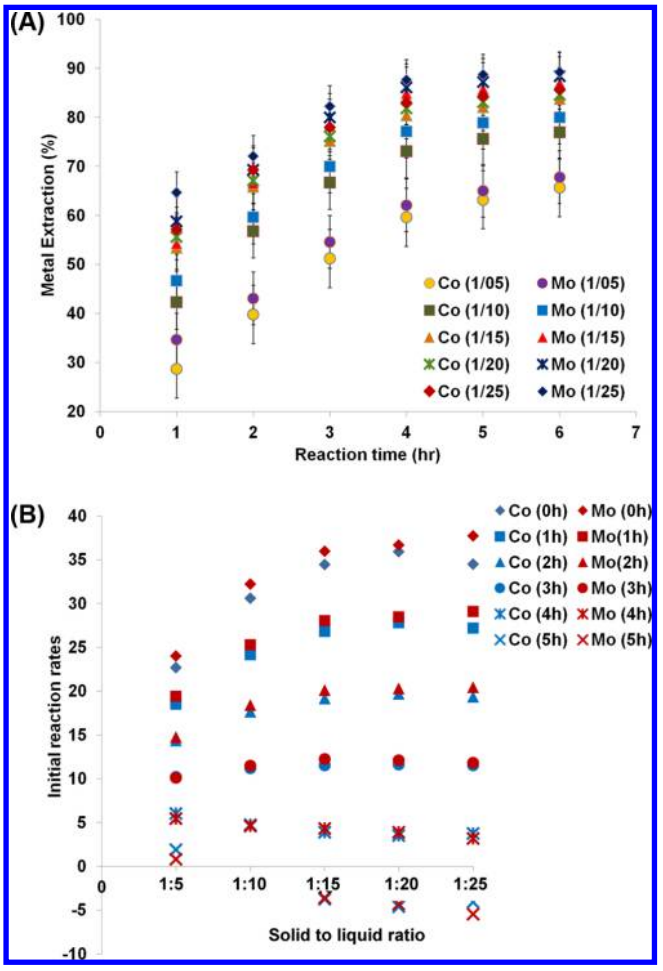

Figure 5. (A) Effect of solid to liquid ratio on metal extraction efficiency. (Reaction conditions: molar concentration of EDTA = 0.4 M, particle size = 100−300 μm, temperature = 120 °C, time = 4 h, stirring speed = 400 rpm, pH = 9). (B) Plot of initial reaction rate vs solid to liquid ratio.

higher initial reaction rate to maximize the extraction of Co and Mo metals.

3.4. Effect of Reaction pH on Metal Extraction. Reaction pH was varied from pH = 7−11 to maximize the amount of metal extracted from spent catalyst. Figure 6 depicts the effect of reaction pH on extraction efficiency of chelating agent EDTA to extract Co and Mo. Few experiments were also performed with biodegradable chelating agent [*S*,*S*]-EDDS to compare the extraction efficiency of these two chelating agents and to investigate the favorable pH range for the extraction process using both chelating agents, however due to high cost of chelating agent [*S*,*S*]-EDDS, it was not used for all extraction experiments. It may be seen from the Figure 6 that with the increase in reaction pH from pH = 7 to 10, an increase in Co and Mo extraction was observed using EDTA, whereas at pH = 10, no significant increase in extraction efficiency was seen. Similar trends were observed in case of biodegradable chelating agent [*S*,*S*]-EDDS, however, the favorable pH range for the reaction was narrow and no significant increase in extraction efficiency was demonstrated beyond pH = 8. It was observed that [*S*,*S*]-EDDS can extract higher amount of metals even at neutral pH whereas EDTA could not show significant extraction efficiency at pH = 7. Similar observations have been reported in literature where [*S*,*S*]-EDDS was used for

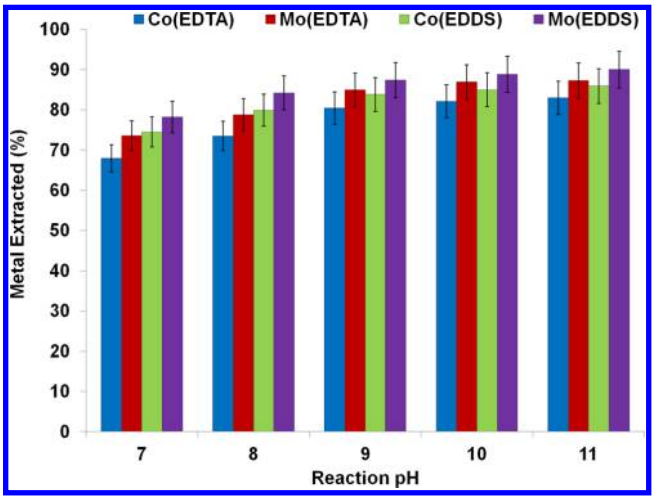

Figure 6. Effect of reaction pH on extraction efficiency (Reaction conditions: molar conc. of EDTA = 0.4 M, S/L = 1/15, temperature = 120 °C, time = 4 h, stirring speed = 400 rpm, particle size = 100−300 μ).

nickel extraction from spent catalyst and the statistical optimization using response surface methodology suggested pH = 7 as the optimized pH for the reaction.[20]

The reason behind this difference in pH range and effect of pH on extraction efficiency may be explained from A and B of Figure 7 where the percentage distribution of different protonation stages of EDTA and [*S*,*S*]-EDDS are shown. An autogenous pH is generated due to displacement of hydrogen

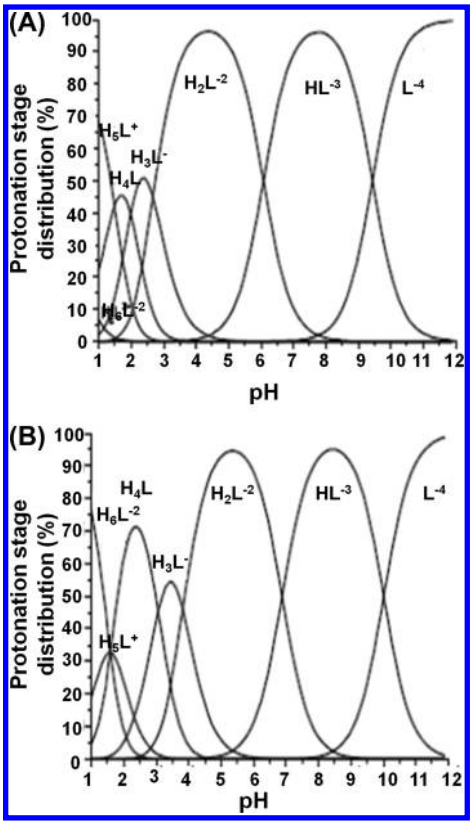

Figure 7. (A) (%) Distribution of various protonation stages of EDTA[24] (B) (%) Distribution of various protonation stages of [*S*,*S*]-EDDS.[24]

dx.doi.org/10.1021/ie4024484 | *Ind. Eng. Chem. Res.* XXXX, XXX, XXX−XXX

Table 2. Analysis of Various Physical Properties of Different Samples Using BET and Density Measurement Method

samples	BET surface area (m^2/g)	pore volume (cm^3/g)	pore diameter (nm)	density (g/cm^3)
fresh catalyst	188.43 ± 1.5	0.39 ± 0.3	8.2 ± 0.5	1.02 ± 0.2
SC	91.87 ± 0.4	0.18 ± 0.1	11.1 ± 1	1.16 ± 0.3
R-1cycle	115.07 ± 1.5	0.21 ± 0.2	12.1 ± 1	1.08 ± 0.2
R-2cycle	157.88 ± 1.4	0.27 ± 0.3	6.4 ± 0.6	0.96 ± 0.06
WR	196.49 ± 2	0.48 ± 0.5	9.1 ± 1	0.78 ± 0.04
synthesized catalyst	163.65 ± 1.5	0.33 ± 0.2	7.9 ± 0.5	1.09 ± 0.2

ion from a protonated form of the chelating agent by a metal ion. This autogenous pH depends on the base strength of the counterions of metal salt.[24] Here in eq 9, the relation between the concentration of free aqua metal ions at equilibrium (pM) and reaction pH is shown:[24]

$$\mathrm{pM} = n\mathrm{pH} + \frac{\log([\mathrm{HL}]^n}{[\mathrm{ML}_n^{(x-n)}]} + \log K{*}K_a{}^n \quad (9)$$

where L refers to ligand, HL corresponds to the protonated form of the chelating agent, ML is metal chelate complex, n is slope of the curve, and K and K_a are the stability constants. It is necessary to understand the various protonated forms of EDTA and to distinguish between the conjugate base ($EDTA^{-4}$) and precursor to the ligand (H_4EDTA) to benefit from the effect of reaction pH in extraction efficiency of the chelating agent.

At the most acidic pH value (pH = 1−2), the fully protonated H_6EDTA^{2+} form predominates, whereas at the alkaline pH above pH = 10, the fully deprotonated L^{4-} form is prevalent as demonstrated in Figure 7A. It can be depicted from Figure 7A that within the pH range 2−6, the free form of EDTA is H_2L^{-2}, which provides the availability of two protons for displacement by metal ion chelation. EDTA exists in the form of HL^{-3} between pH = 6−10; therefore, the slope of the curve changes to 1, and only one proton can be displaced. Thus, up to pH = 10, the rise of pM with an increase in pH shows the increase in the degree of metal binding due to hydrogen displacement. Above pH = 10, chelates are formed from fully dissociated chelant $L^{-4,}$ where no hydrogen ions are displaced and the slope of the curve is zero; therefore, above pH = 10, pM is independent of pH. Accordingly, the extraction efficiency of EDTA does not depend on the reaction pH beyond pH = 10; thus, no significant increase was observed in metal extraction at pH = 11. A similar description is applicable for the chelating agent [*S*,*S*]-EDDS as shown in Figure 7B where fully protonated forms (H_6L^{+2}, H_5L^{+}) exist at very low pH values, while the HL^{-3} protonated form exists predominantly between pH = 8 and pH = 9; therefore, the maximum effect of reaction pH was observed in this range, while above pH = 9, no significant improvement in extraction efficiency was seen.[24]

Thus, considering all the mass transfer limitations (effect of stirring speed and particle size distribution), kinetic aspects (reaction temperature, reaction time, molar concentration of EDTA, and S/L ratio) of the reaction and effect of reaction pH, the optimum reaction conditions for the chelant-assisted extraction process are as follows: stirring speed = 400 rpm, particle size distribution = 100−300 μm, reaction temperature = 120 °C, reaction time = 4 h, molar concentration of EDTA = 0.4 M, S/L = 1/15, and reaction pH = 9. Maximum percentages of 88% Co and 91.1% Mo were extracted in two process cycles, while at the optimum reaction conditions, 80.4% Co and 84.9% Mo could be recovered from the spent catalyst.

3.5. Recycling of Chelating Agent EDTA. Recovery and recycling of chelating agent EDTA make the chelant-assisted metal extraction process more favorable than other traditional approaches such as leaching, adsorption, roasting, etc. Dechelation was carried out at ambient room temperature over an 8 h period as described in the literature.[14] About 96% EDTA was recovered during the dechelation process. The metal solution was then kept under cold conditions for 2 days to precipitate the remaining EDTA. Under such conditions, an additional 1% of the EDTA was recovered. However, nearly 2−3% of the EDTA was lost in the metal solution because of its inherent solubility.

Extraction efficiency of recovered EDTA was investigated for up to five cycles to benefit from the substantial recycling of the chelating agent, EDTA. Significant metal extraction efficiency was observed with the recovered EDTA at optimum reaction conditions (Figure 3 in SI). The percentage extractions of Co and Mo were 78.8% and 82.6% after the second cycle. Nevertheless, after the fifth cycle operation, approximately 20% less extraction efficiency was observed than with fresh EDTA; consequently, no further experiments were carried out using recovered EDTA. Characterization (NMR and FT-IR) of fresh and recovered EDTA(s) were performed to find out the reason behind the loss in extraction efficiency of recovered EDTA. Loss in peak area and intensity was observed in the NMR spectra for recovered EDTA (Figure 4 in SI) which reflects the loss in the number of metal-binding sites due to repetitive precipitation of EDTA. Variation of the wave numbers for fresh EDTA and recovered EDTA(s) was also observed in the FT-IR spectra (Figure 5 in SI). It is apparent from the NMR and FT-IR spectra that due to the increase in impurities with each recycling operation of EDTA, extraction efficiency of EDTA decreased and therefore, it is advisable not to recycle EDTA after four chelation cycles to maintain the economic consistency of the process. Efforts are still going on to minimize the loss in extraction efficiency by finding ways to improve the properties of recovered EDTA.

3.6. Recovery and Recycling of Extracted Metals. Recycling of the extracted heavy metals is the key feature of the present research work. Chelation experiments were performed to extract heavy metals Co and Mo from spent catalyst (SC). The recovered support material, obtained after the first cycle of the chelation process (R-1cycle), was recycled to extract the remaining amount of heavy metals from the residue. The residue, obtained after the second cycle (R-2cycle), was washed five times using 25 mL of distilled water for every wash and calcined at 300 °C for 3 h to remove any volatile impurities. The extracted metals, Co and Mo, and the support material, alumina, were investigated for the possibility of their recycling in the preparation of new, fresh catalyst. Synthesis of new catalyst was performed using the incipient wet impregnation method where the residue material obtained after washing (WR) was reused as a support; solution obtained after the

dx.doi.org/10.1021/ie4024484 | Ind. Eng. Chem. Res. XXXX, XXX, XXX−XXX

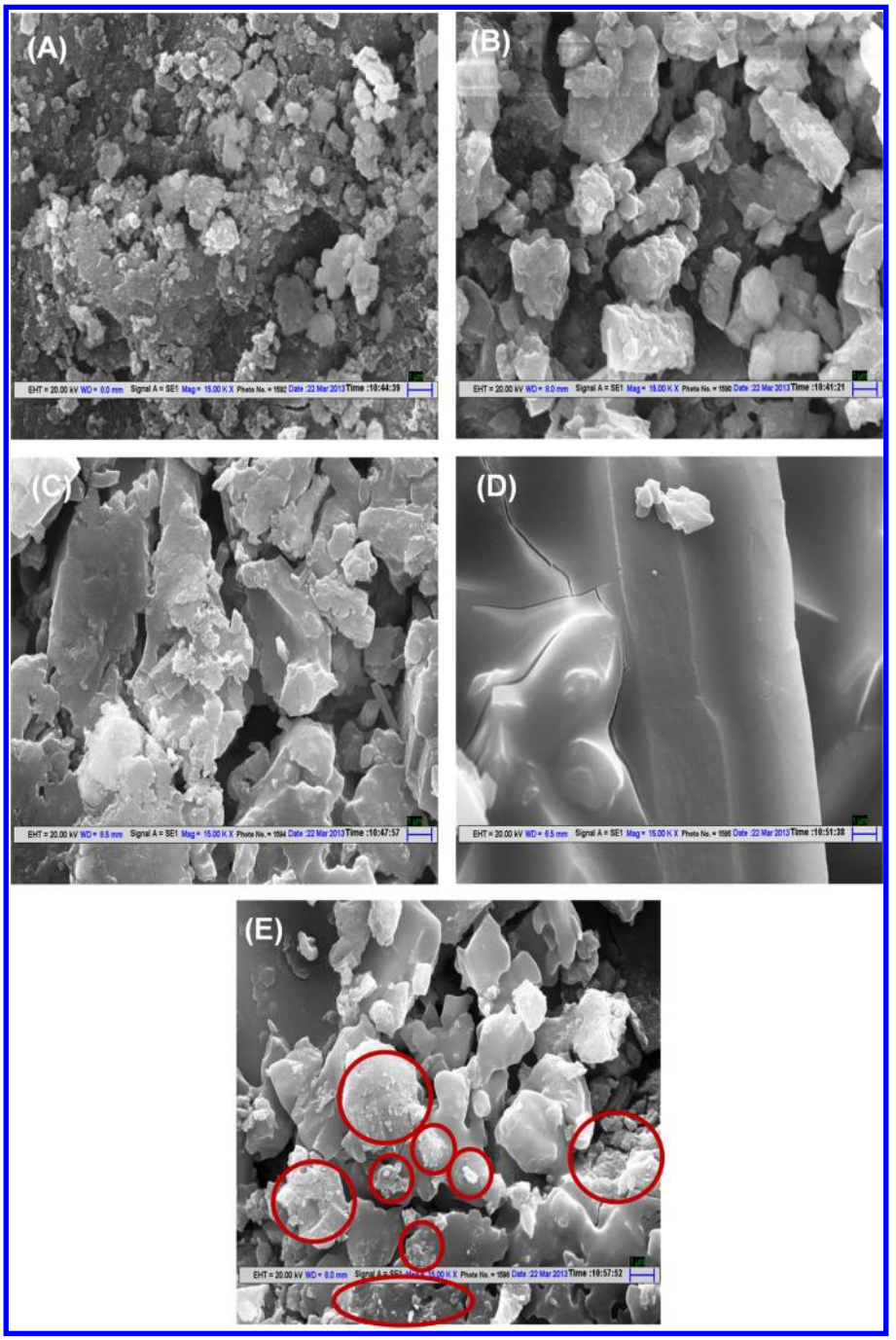

Figure 8. (A) SEM analysis of spent catalyst. (B) SEM analysis of recovered support material after first cycle (R-1). (C) SEM analysis of recovered support material after second cycle (R-2). (D) SEM analysis of washed residue (WR). (E) SEM analysis of synthesized catalyst.

dechelation and filtration process was used to impregnate the extracted Co and Mo metals. Various characterization procedures were adopted to investigate the physical properties of SC, R-1cycle, R-2cycle, WR, and synthesized catalyst using recovered metals.

3.6.1. Analysis of Physical Properties (Surface Area, Pore Volume, Pore Diameter, Density). Brunauer−Emmett−Teller surface area (BET) measurement was conducted using Micromeritics adsorption equipment (ASAP 2010) to determine specific surface area of all the samples using liquid nitrogen of 99.99% purity. Samples were kept in the oven at 110 °C for 12 h in order to remove the moisture. The dried samples were degasified under nitrogen atmosphere followed by analysis of the surface area. Densities of each sample were also evaluated using tapping method. Table 2 indicates the BET surface area, pore volume, pore diameter, and density of fresh catalyst, spent catalyst, and recovered support material obtained after different cycles and synthesized catalyst. It may be understood from Table 2 that surface area of R-1cycle is higher than SC due to extraction of some amount of heavy metals present in SC and void channel formation that takes place in R-1cycle. However, the increase in surface area was not significant after the first chelation cycle which may correspond to the presence of unextracted metal particles, some impurities such as sulfur, EDTA, volatile components, etc. on the residue surface which may still clog the pores. However, in the case of R-2cycle,

dx.doi.org/10.1021/ie4024484 | *Ind. Eng. Chem. Res.* XXXX, XXX, XXX−XXX

most of the metal was extracted from the spent catalyst, and alumina was left as major component in R-2cycle. Therefore, the surface area is higher than the previous two samples, while the density decreases due to a lower amount of metal particles in R-2cycle than in SC and R-1cycle. Structural analysis of WR demonstrates the highest surface area among all the samples, and hence, the lowest density was also observed in the case of WR. It may be explained by the fact that impurities such as EDTA, some remaining unextracted metal, sulfur, volatile components, etc. were removed during water washing, and only alumina was left in the washed residue. Therefore, the pore volume increases, and particle surface area also increases. It was also observed that the surface area of the synthesized catalyst is less than that of the washed residue and density increases which clearly depicts the metal impregnation on the support material for the synthesis of fresh catalyst. Comparison of physical properties of lab-synthesized catalyst with those of fresh catalyst suggest lower surface area and pore volume of lab-synthesized catalyst as compared to those of the fresh catalyst. The observation could be justified with the fact that the γ-alumina was used as the support material in fresh catalyst; however, the temperature and time treatment of the extraction process may cause several phase transformations in the catalyst material which may change phase crystallinity and particle size. Therefore, the β-alumina phase of the support material could be recovered in a chelant-assisted metal extraction process after the second chelation cycle. β-Alumina has a smaller surface area as compared to that of the γ-alumina; thus, the difference in the surface area between fresh and synthesized catalyst could be seen as shown in Table 2. However, regaining the crystallinity and surface area of the support material alumina is part of ongoing research.

3.6.2. Scanning Electron Microscopic (SEM) Analysis. Scanning electron microscopic (SEM) analysis was used to study the morphology of catalyst and residues. Sample preparation was done as explained in the literature.[12] The SEM analysis was performed at magnification of 15000× to investigate the change in morphology of spent catalyst, R-1cycle, R-2cycle, WR and synthesized catalyst. Agglomeration of particles, lump formation, and nonuniform distribution of metals were seen in the SEM image of spent catalyst as shown in Figure 8A. It may be due to catalyst deactivation and coke formation at the catalyst surface. Figure 8B shows the morphology of R-1cycle where void channel formation can be seen due to release of metal content from spent catalyst which helps to increase the number of active sites for reaction. However, some impurities were also observed on the surface due to the presence of EDTA, volatiles, and sulfur content. Figure 8C shows the microscopic image of the R-2cycle where a clear background with a lower amount of metal content confirms the Co and Mo extraction from spent catalyst after the second cycle. However, volatiles and some other impurities were still present in the R-2cycle which need to be removed to make the residue appropriate for using as a support material in catalyst preparation. Therefore, the morphology of the washed residue was also investigated, and it is clear from Figure 8D that washed residue does not contain any impurities and a more uniform surface was observed than in the R-2cycle. The morphology of the synthesized catalyst (as shown in Figure 8E) confirms the impregnation of extracted metal Co and Mo on the support. The area has been encircled in the figure where impregnated metal on the support can be seen clearly.

Energy dispersive X-ray analysis was also performed for all the samples. It was concluded from the analysis that spent catalyst contains the peaks for Mo, Co, Al, and Mg as the predominant elements. Co and Mg peaks were not seen in the R-1cycle, whereas peak intensity for Mo was lesser than in the SC. The R-2cycle and washed residue showed similar metal distribution in EDX spectra, and peak intensity for Mo was observed to be negligible. Peak intensity for aluminum metals was highest in support material after washing and calcination which confirmed the predominance of alumina in the recovered support material. EDX spectra of the synthesized catalyst demonstrated peaks for Co and Mo, with significant intensity along with a strong peak for aluminum, which evidence the successful impregnation of extracted metals on the support.

3.6.3. X-ray Diffraction Analysis (XRD). X-ray diffraction (XRD) analysis was performed at a step size of 0.05° and a count time of 1 s per step over the range $10° < 2\theta < 90°$ to identify the crystalline phases of catalyst and residue samples. Phases were identified using the Joint Committee on Powder Diffraction Standards (JCPDS) software. XRD patterns for SC, R-1cycle, R-2cycle, WR, and synthesized catalyst are shown in Figure 9. A strong peak at 2θ of 46.36° representing the (112)

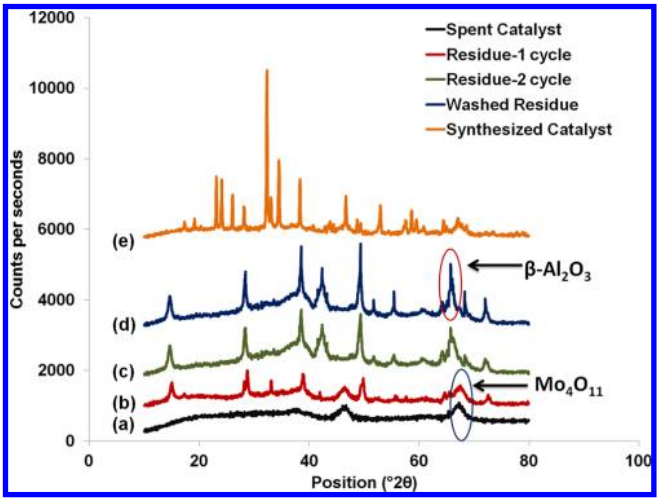

Figure 9. (a–e) XRD patterns for spent catalyst, residues, and synthesized catalyst.

monoclinic primitive plane of molybdenum oxide (MoO_3), can be clearly seen in spent catalyst procured from the hydrodesulfurization unit as shown in Figure 9a. In addition, another broad peak near 2θ of 66.80° was observed for the $Al_2(MoO_4)_3$ species, rather than the MoO_3 species, which can be attributed to the diffraction of the (131) plane. Figure 9b represents the XRD pattern for sample R-1cycle, in which relatively weak diffraction peaks related to molybdenum oxides are detected at 2θ = 33.09 and 46.73°. The highest peak with 100% relative intensity was observed at an angle of 28.75° for the peak $Al_2(MoO_4)_3$. Some diffraction peaks were also observed for aluminum oxide (β-alumina) near 2θ of 14.98° and 38.91° which depicts the predominance of alumina peaks in the recovered support material. The XRD patterns for sample R-2cycle and washed residue were found to be very similar and shown in c and d of Figure 9, respectively. Aluminum oxide (β-Al_2O_3) was observed as the major component in both the samples, and sharp peaks were obtained at angle 2θ of 14.77°, 38.62°, 55.54°, 65.04°. One weak peak was observed for MoO_3 at 2θ of 33.09°, and another peak at 2θ of 49.51° was observed

dx.doi.org/10.1021/ie4024484 | Ind. Eng. Chem. Res. XXXX, XXX, XXX–XXX

for $Al_2(MoO_4)_3$. Thus, weak diffraction peaks for Mo(VI) component and the absence of any peak for the Co(II) component confirms the extraction of these two metals from the spent catalyst. The synthesized catalyst, using recovered support material aluminum oxide and extracted metals in solution, confirms the presence of $CoMoO_4$ (2θ = 44.40°), Mo_9O_{26} (2θ = 32.32°, 46.68°), MoO_3 (2θ = 23.12°, 26.05°); weak peaks of Mo_4O_{11} (2θ = 33.03, 52−57°) and $Al_2(MoO_4)_3$ within the range of 2θ = 60.81−68.43° in the XRD pattern (as shown in Figure 9e) corroborate the successful metal impregnation on the recovered support material. Various XRD phases obtained from Figure 9 along with their *d*-spacing, *h*,*k*,*l* values, crystal structure, and JCPDS number are listed in Table 3.

Table 3. XRD Analysis of Different Phases Present in SC, R-1cycle, R-2Cycle, WR, and Synthesized Catalyst

phases	*d*-spacing	*h*, *k*, *l*	crystal structure	JCPDS No.
		Spent Catalyst		
MoO_3	1.95678	1 1 2	monoclinic primitive	85−2405
$Al_2(MoO_4)_3$	1.3953	1 3 1	orthorhombic primitive	85−2286
		R-1Cycle		
$Al_2(MoO_4)_3$	3.1022	1 2 2	orthorhombic primitive	85−2286
	1.8316	4 4 0		
Mo_8O_{23}	2.7019	0 0 6	monoclinic primitive	84−1247
β-Al_2O_3	2.3124	3 1 0	monoclinic end-centered	86−1410
	5.7264	2 0 0		
		R-2Cycle/WR		
β-Al_2O_3	5.7281	2 0 0	monoclinic end-centered	86−1410
	2.3193	3 1 0		
	1.6513	5 1 2		
Al_2O_3	1.3928	2 1 4	hexagonal rhombocentered	85−1337
$Al_2(MoO_4)_3$	1.8346	4 4 0	monoclinic primitive	84−1652
		Synthesized Catalyst		
MoO_3	3.8437	1 0 0	monoclinic primitive	85−2405
	3.4167	0 1 2		84−1360
Mo_9O_{26}	2.7636	4 2 4	monoclinic end-centered	84−1466
	1.9449	4 4 0		
Mo_4O_{11}	2.7180	0 2 0	monoclinic primitive	86−1269
	3.1656	2 0 2		
	2.3465	2 0 8		
	1.6004	4 1 1		
	1.5732	2 3 3		
	1.5522	4 1 5		
$Al_2(MoO_4)_3$	1.52190	7 1 3	orthorhombic primitive	85−2286
	1.4443	2 6 1		
$CoMoO_4$	2.0345	1 1 2	monoclinic primitive	86−0363

ICP-OES analysis also support the above observations depicted from characterization of SC, R-1cycle, R-2cycle, WR, and synthesized catalyst. It was demonstrated in the ICP-OES results that recovered support material after washing contained nearly 96% aluminum and 4% other impurities. Nearly 1% Co(II) and 5.7% Mo(VI) was observed in the synthesized catalyst with the β-alumina as support material.

Thus, characterization studies (BET, XRD, SEM, EDX, and ICP-OES) for different samples corroborate the recovery and recycling of heavy metals for the synthesis of a new catalyst of commercial importance. The recycling aspect of the extracted metals provides the chelant-assisted metal extraction process a more viable direction toward waste minimization by utilizing it in other important chemical processes, reforming the reaction and steel industries.

4. INCENTIVES FOR USING CHELANT-ASSISTED EXTRACTION METHODOLOGY

The proposed methodology for chelant-assisted extraction of heavy metals offers an environmentally benign approach for waste management. A number of hydrometallurgical approaches have been reported in literature for metal recovery from spent catalyst and have been listed here in Table 4. These methods include acid and alkali leaching followed by selective precipitation or an ion exchange process to achieve individual metals. Significant metal recoveries have been reported in the literature that use acid-/alkali-leaching processes (as shown in Table 4); however, acid is hazardous to handle at higher temperature, and it cannot be recovered and reused in the process. Leaching is carried out at high temperature; therefore, generation of corrosive environment and the necessity for expensive material of construction are other concerns associated with the acid-leaching process. Bioleaching has also emerged as a promising technology for recovering metals from waste material in recent years; however, longer leaching time to achieve extraction efficiencies conquers its importance for metal extraction. The associated risk of contamination and less acceptability of microorganisms at high temperatures are other important factors to consider while employing biotechnological approaches. The literature suggests some solvent extraction methods for selective precipitation of metals; nevertheless, large amounts of chemicals used in the process, disposal of these chemicals, and the possibility of secondary pollution by these chemicals may prohibit the utility of these methods in industrial practice.

Chelation technology has been employed for the first time in this study for the extraction of heavy metals from multimetal spent catalysts. It can be seen from Table 4 that extraction of heavy metals using the chelating agent can give extraction efficiency comparable with that of other conventional methodology. It offers certain incentives to industrial practice as an ecofriendly approach by recovering chelating agents and recycling it for another cycle, thus minimizing the amount of solid wastes and toxic discharge into the atmosphere. The process can be easily implemented in the lab due to the absence of any hazardous chemicals and byproducts. The high efficiency of metal extraction, high thermodynamic stabilities of the metal complexes, low adsorption of the chelating agent to the catalyst, and minor impacts on the physical and chemical properties of the solid matrix as compared to the effects of acids make chelant-assisted extraction methodology more convincing than other available methods which have been reported in the literature.

5. CONCLUSION

The present study is a successful demonstration of industrial waste minimization and development of an ecofriendly technology for recovery of heavy metals. Transport of the metal−chelate complex and the dissolution of target metals in aqueous medium were investigated by varying different process parameters. A pH-controlled precipitation method was found to be a feasible approach for separation of individual metals from the solution. Cobalt was precipitated at alkaline pH, and then molybdenum was precipitated at acidic pH to maximize the metal extraction and to avoid coprecipiation. The

dx.doi.org/10.1021/ie4024484 | Ind. Eng. Chem. Res. XXXX, XXX, XXX−XXX

Table 4. Comparative Analysis of Various Conventional Methods with the Proposed Chelant-Assisted Extraction Methodology

catalyst source	metals present	method of metal extraction	extraction efficiency	refs
sulfuric acid production unit	V, K, Fe, Si	leaching using urea solution	V (78%), K (90%), and Fe (29%)	25
spent petroleum catalyst	Ni, V, Mo	leaching with $(NH_4)_2CO_3$ followed by washing with H_2SO_4	Ni (90−93%), Mo (12−25%), and V(50−61%)	7
spent petroleum catalyst	Ni, V, Mo	acid leaching (H_2SO_4)	Ni and V (more than 95%), Mo (28%)	7
spent hydroprocessing catalyst	Ni, V, Mo	bioleaching using iron/sulfur oxidizing bacteria	Ni (83%), V (90%), Ni and V (50%) in absence of iron; Mo (30−40%)	26
spent hydro-desulfurization catalyst	Ni, Mo, V	acid leaching + electrolysis process	Mo (14%), Ni (60%) and V (65%)	27
spent hydrotreating catalysts	CoMo and NiMo/Al_2O_3	H_2SO_4 leaching + solvent extraction + ion exchange	Mo (>99.5wt.%), Ni and Co (98.0 ± 0.3 wt.%)	28
spent hydro-desulfurization catalyst	Ni, Mo, V, Al	leaching using oxalic acid solution with H_2O_2 addition	Mo (90%),V (94%), Ni (65%) and Al (33%)	8
petroleum refining industry	Ni−Mo/ γ-Al_2O_3	alkali leaching (Na_2CO_3/H_2O_2)	Mo (>99%) with 99.4% purity, Ni and Al (88%)	29
spent refinery processing catalyst	Ni, Mo, Al	bioleaching (*Aspergillus niger*)	Ni (78.5%), Mo (82.3%) and Al (65.2%)	30
hydro-desulfurization spent catalyst	Co, Mo, Al	chelation technology using EDTA as chelating agent	Co (80.4%), Mo (84.9%) with 91% purity	present study

dissolution and separation processes employed in this work are relatively low-energy intensive with respect to the traditional pyro/hydrometallurgical processes and chlorination procedures reported in the literature for processing spent HDS catalysts. Co (80.4%) and Mo (84.9%) were extracted from the spent hydrodesulfurization catalyst using the chelating agent EDTA under optimum reaction conditions. The conclusion regarding optimum parameters is based on the experimental results for maximizing the extraction efficiency, as well as the economical feasibility of the process. The biodegradable chelating agent [*S*,*S*]-EDDS showed extraction efficiency similar to that of EDTA for a relatively narrower pH range than that for EDTA; however, the high capital cost of [*S*,*S*]-EDDS restricts its pertinency for commercial application. Successful recovery and recycling of recovered chelating agent EDTA for metal extraction minimizes the EDTA mobilization in the environment. Recyling of extracted metals and recovered support material in the synthesis of new catalyst is another apprizing factor of this process which makes this extraction process more convincing for industrial practice. Therefore, the proposed chelant-assisted metal extraction technology can be considered an environmentally benign approach to recover and reutilize the heavy metals present in waste material.

■ ASSOCIATED CONTENT

Ⓢ Supporting Information

Additional Figures as described in the text. This material is available free of charge via the Internet at http://pubs.acs.org.

■ AUTHOR INFORMATION

Corresponding Author

*E-mails: nigamkdp@gmail.com; drkdpn@gmail.com. Telephone/Fax: +91-11-26591020.

Notes

The authors declare no competing financial interest.

■ REFERENCES

(1) United Nations Environment Programme, Responsible Resource Management for a Sustainable World: Findings from the International Resource Panel, 2012. ISBN:978-92-807-3278-8. http://www.unep.org/resourcepanel/Portals/24102/SYNOPSIS%20Final%20compressed.pdf, April 24, 2013.

(2) Shariat, M. H.; Setoodeh, N.; Dehghan, R. A. Optimizing conditions for hydrometallurgical production of purified molybdenum trioxide from roasted molybdenite of sarcheshmeh. *Miner. Eng.* **2001**, *14*, 815.

(3) Sun, D. D.; Tay, J. H.; Cheong, H. K.; Leung, D. L. K.; Qian, G. Recovery of heavy metals and stabilization of spent hydrotreating catalyst using a glass−ceramic matrix. *J. Hazard. Mater.* **2001**, *B87*, 213.

(4) Kar, B. B.; Datta, P.; Misra, V. N. Spent catalyst: secondary source for molybdenum recovery. *Hydrometallurgy.* **2004**, *72*, 87.

(5) Kar, B. B.; Murthy, B. V. R.; Misra, V. N. Extraction of molybdenum from spent catalyst by salt roasting. *Int. J. Miner. Process.* **2005**, *76*, 143.

(6) Kim, D. J.; Mishra, D.; Ahn, J. G.; Chaudhury, G. R.; Ralph, D. E. A novel process to treat spent petroleum catalyst using sulfur-oxidizing lithotrophs. *J. Environ. Sci. Health A* **2009**, *44*, 1585.

(7) Mishra, D.; Chaudhary, G. R.; Kim, D. J.; Ahn, J. G. Recovery of metal values from spent catalyst using leaching-solvent extraction technique. *Hydrometallurgy.* **2010**, *101*, 35.

(8) Mulak, W.; Szymczycha, A.; Lesniewicz, A.; Żyrnicki, W. Preliminary results of metals leaching from a spent hydrodesulphurization (HDS) catalyst. *Physicochem. Probl. Miner. Process.* **2006**, *40*, 69.

(9) Zeng, Li.; Cheng, C. Y. Recovery of molybdenum and vanadium from synthetic sulphuric acid leach solutions of spent hydro-desulphurisation catalysts using solvent extraction. *Hydrometallurgy* **2010**, *101*, 141.

(10) Park, K. H.; Reddy, B. R.; Mohapatra, D.; Nam, C. W. Hydrometallurgical processing and recovery of molybdenum trioxide from spent catalyst. *Int. J. Miner. Process.* **2006**, *80*, 261.

(11) Santhiya, D.; Ting, Y. P. Bioleaching of spent refinery processing catalyst using Aspergillus Niger with high-yield oxalic acid. *J. Biotechnol.* **2005**, *116*, 171.

(12) Chauhan, G.; Pant, K. K.; Nigam, K. D. P. Extraction of nickel from spent catalyst using biodegradable chelating agent EDDS. *Ind. Eng. Chem. Res.* **2012**, *51*, 10354.

(13) Goel, S.; Pant, K. K.; Nigam, K. D. P. Extraction of nickel from spent catalyst using fresh and recovered EDTA. *J. Hazard. Mater.* **2009**, *171*, 253.

(14) Vuyyuru, K. R.; Pant, K. K.; Krishnan, V. V.; Nigam, K. D. P. Recovery of nickel from spent industrial catalysts using chelating agents. *Ind. Eng. Chem. Res.* **2010**, *49*, 2014.

(15) Nowack, B. Environmental chemistry of aminopolycarboxylate chelating agents. *Environ. Sci. Technol.* **2002**, *36*, 4009.

(16) Yip, T. C. M.; Tsang, D. C. W.; Lo, I. M. C. Interactions of chelating agents with Pb-goethite at the solid−liquid interface: Pb extraction and re-adsorption. *Chemosphere* **2010**, *81*, 415.
(17) Lo, I. M. C.; Tsang, D. C. W.; Yip, T. C. M.; Wang, F.; Zhang, W. Significance of metal exchange in EDDS-flushing column experiments. *Chemosphere* **2011**, *83*, 7.
(18) Zhang, W.; Tsang, D. C. W. Conceptual framework and mathematical model for the transport of metal−chelant complexes during in situ soil remediation. *Chemosphere* **2013**, *91*, 1281.
(19) Devi, C. H. K.; Krishna, D. G.; Devanna, N.; Chandrasekhar, K. B. Direct and derivative spectrophotometric determination of Molybdenum (VI) in presence of micellar medium in food stuffs, pharmaceutical samples and in alloys using cinnamaldehyde-4-hydroxy benzoylhydrazone (CHBH). *Res. J. Pharm. Biol. Chem. Sci.* **2010**, *1*, 808.
(20) Chauhan, G.; Pant, K. K.; Nigam, K. D. P. Development of green technology for extraction of nickel from spent catalyst and its optimization using response surface methodology. *Green Process. Synth.* **2013**, *2*, 259.
(21) Huang, J. H.; Kargl-Simard, C.; Oliazadeh, M.; Alfantazi, A. M. pH −Controlled precipitation of cobalt and molybdenum from industrial waste effluents of a cobalt electrodeposition process. *Hydrometallurgy* **2004**, *75*, 77.
(22) De Lima, T. S.; Campos, P. C.; Afonso, J. C. Metals recovery from spent hydrotreatment catalysts in a fluoride-bearing medium. *Hydrometallurgy* **2005**, *80*, 211.
(23) Beckstead, L. W.; Huggins, D. K.; Chou, E. C. Precipitation of molybdenum sulfide from aqueous solution. *JOM-J Met.* **1985**, *37*, 42.
(24) Hyvonen H. Studies on metal complex formation of environmentally friendly aminopolycarboxylate chelating agents, Academic Dissertation, Department of Chemistry, Univeristy of Helsinki, Finland, 2008. .
(25) Mazurek, K.; Białowicz, K.; Trypuć, M. Recovery of vanadium, potassium and iron from a spent catalyst using urea solution. *Hydrometallurgy* **2010**, *103*, 19.
(26) Beolchini, F.; Fonti, V.; Ferella, F.; Vegliò, F. Metal recovery from spent refinery catalysts by means of biotechnological strategies. *J. Hazard. Mater.* **2010**, *178*, 529.
(27) Lai, Y. C.; Lee, W. J.; Huang, K. L.; Wu, C. M. Metal recovery from spent hydrodesulfurization catalysts using a combined acid-leaching and electrolysis process. *J. Hazard. Mater.* **2008**, *154*, 588.
(28) Valverde, I. M., Jr.; Paulino, J. F.; Afonso, J. C. Hydrometallurgical route to recover molybdenum, nickel, cobalt and aluminium from spent hydrotreating catalysts in sulfuric acid medium. *J. Hazard. Mater.* **2008**, *160*, 310.
(29) Park, K. H.; Mohapatra, D.; Reddy, B. R. Selective recovery of molybdenum from spent HDS catalyst using oxidative soda ash leach/carbon adsorption method. *J. Hazard. Mater.* **2006**, *B138*, 311.
(30) Santhiya, D.; Ting, Y. P. Use of adapted *Aspergillus niger* in the bioleaching of spent refinery processing catalyst. *J. Biotechnol.* **2006**, *121*, 62.